

Musculoskeletal architecture of the prey capture apparatus in salamandrid newts with multiphasic lifestyle: does anatomy change during the seasonal habitat switches?

Egon Heiss,¹ Stephan Handschuh,² Peter Aerts^{3,4} and Sam Van Wassenbergh^{3,5}

¹*Institute of Systematic Zoology and Evolutionary Biology, Friedrich-Schiller-University Jena, Jena, Germany*

²*VetCore Facility for Research, Imaging Unit, University for Veterinary Medicine Vienna, Vienna, Austria*

³*Department of Biology, University of Antwerp, Antwerp, Belgium*

⁴*Department of Movement and Sports Sciences, Ghent University, Ghent, Belgium*

⁵*Evolutionary Morphology of Vertebrates, Ghent University, Ghent, Belgium*

Abstract

Some newt species change seasonally between an aquatic and a terrestrial life as adults, and are therefore repeatedly faced with different physical circumstances that affect a wide range of functions of the organism. For example, it has been observed that seasonally habitat-changing newts display notable changes in skin texture and tail fin anatomy, allowing one to distinguish an aquatic and a terrestrial morphotype. One of the main functional challenges is the switch between efficient aquatic and terrestrial prey capture modes. Recent studies have shown that newts adapt quickly by showing a high degree of behavioral flexibility, using suction feeding in their aquatic stage and tongue prehension in their terrestrial stage. As suction feeding and tongue prehension place different functional demands on the prey capture apparatus, this behavioral flexibility may clearly benefit from an associated morphological plasticity. In this study, we provide a detailed morphological analysis of the musculoskeletal system of the prey capture apparatus in the two multiphasic newt species *Ichthyosaura alpestris* and *Lissotriton vulgaris* by using histological sections and micro-computed tomography. We then test for quantitative changes of the hyobranchial musculoskeletal system between aquatic and terrestrial morphotypes. The descriptive morphology of the cranio-cervical musculoskeletal system provides new insights on form and function of the prey capture apparatus in newts, and the quantitative approach shows hypertrophy of the hyolingual musculoskeletal system in the terrestrial morphotype of *L. vulgaris* but hypertrophy in the aquatic morphotype of *I. alpestris*. It was therefore concluded that the seasonal habitat shifts are accompanied by a species-dependent muscular plasticity of which the potential effect on multiphasic feeding performance in newts remains unclear.

Key words: environmental transitions; feeding; lissamphibia; urodeles.

Introduction

Some newt species (salamandrids) show a multiphasic lifestyle where adults change seasonally between aquatic and terrestrial habitats (Matthes, 1934; Denoël, 2004). These multiple environmental transitions are challenging for the whole organism, and are associated with major morphological, physiological and behavioral changes to account for

the different physical properties of water and air (Griffiths, 1997; Thiesmeier & Schulte, 2010). Accordingly, these seasonal shifts between two very different habitats induce notable changes of the whole organism, and result in an aquatic and terrestrial stage with a distinct aquatic and terrestrial morphotype (Matthes, 1934; Halliday, 1974; Nöllert & Nöllert, 1992; Griffiths, 1997; Warburg & Rosenberg, 1997; Denoël, 2004). For example, tail fins grow out in the aquatic stage to increase undulatory swimming performance and are reduced in the terrestrial stage when animals change to quadrupedal locomotion (Nöllert & Nöllert, 1992). Similarly, labial lobes (oral skin folds) are large and well developed in the aquatic stage but are reduced in the terrestrial stage to adapt to the different prey capture modes used in the respective medium (Matthes, 1934).

Correspondence

Egon Heiss, Institute of Systematic Zoology and Evolutionary Biology, Friedrich-Schiller-University Jena, Erbertstr. 1, Jena 07743, Germany.
E: egon.heiss@uni-jena.de

Accepted for publication 29 December 2015

Article published online 19 February 2016

When feeding under water, newts always use suction feeding, involving a fast oropharyngeal expansion that drives prey and surrounding water body to flow into the gaping mouth. In suction feeding, labial lobes occluding the lateral margins of the mouth increase flow velocities and therefore suction feeding performance (Skorczewski et al. 2012; S. Van Wassenbergh & E. Heiss, unpublished data) but are useless on land. For capturing prey on land, newts use a slightly modified suction feeding mode (jaw prehension) and grasp prey by the jaws in their aquatic stage, but they use tongue prehension when in the terrestrial stage. In tongue prehension, the tongue is accelerated out of the mouth to catch prey and to bring it back into the mouth. Accordingly, suction feeding is the prevalent feeding mode in the aquatic stage and tongue prehension the prevalent capture mode used in the terrestrial stage (Heiss et al. 2013, 2015).

However, suction feeding and tongue prehension are fairly different mechanisms and require different specializations of the musculoskeletal system that makes up the prey capture apparatus (Deban, 2003). For example, many hyobranchial muscles that are the main motors powering tongue prehension play a minor role in suction feeding and vice versa. Similarly, the demands on the skeletal elements of the prey capture apparatus, which redirect the muscular forces, differ considerably between suction feeding and tongue prehension (Deban & Wake, 2000; Deban, 2003). In fact, the musculoskeletal arrangement of the prey capture apparatus is different between aquatic and terrestrial salamanders (Deban & Wake, 2000; Wake & Deban, 2000; Deban, 2003). Accordingly, the seasonal switches between habitats in newts that are associated with different prey capture behaviors might demand structural plasticity of the musculoskeletal system to account for the different functional needs in the two different environments.

This hypothesis is based on the fact that adult newts do show structural plasticity exemplified by their seasonal switch between the distinct aquatic and terrestrial morphotypes. For example, fin folds and labial lobes grow when newts change to their aquatic stage and disappear when they leave the water again (Matthes, 1934). Similarly, the structure of the skin changes as the stratum corneum increases in thickness in the terrestrial morphotype (Warburg & Rosenberg, 1997). Structural seasonal changes in the musculoskeletal system, however, have not been studied in any salamanders to date. Nevertheless, such changes are not unlikely as seasonal muscle plasticity was documented previously in other vertebrates where they are associated with seasonally changing functional demands (Flück, 2006; Gerth et al. 2009; Nowell et al. 2011).

In order to improve understanding of form, function and plasticity of the feeding apparatus in newts in the context of their unique multiphasic lifestyle, this study has the following aims: building upon former published work on post-metamorphic salamandrid morphology (Drüner, 1902, 1904; Francis, 1934; Özeti & Wake, 1969;

Findeis & Bemis, 1990) it is first aimed to provide a detailed analysis of the 3D architecture of the complex musculoskeletal system of the prey capture apparatus in two newt species with a multiphasic lifestyle and parallel changing prey capture behavior (Heiss et al. 2013, 2015): *Ichthyosaura alpestris* and *Lissotriton vulgaris*. The 'in situ' analysis of the craniocervical morphology will provide new insights into the integration of skeletal and muscle systems to better understand the complex movement patterns during prey capture. Second, we test for quantitative differences in the musculoskeletal hyobranchial system between the aquatic and the terrestrial morphotypes of *I. alpestris* and *L. vulgaris*. Given that salamanders in general are known for their extraordinary capability of structural plasticity and regeneration capacity (Piatt, 1955; Stocum & Dearlove, 1972; Yokoyama, 2008), quantitative changes as a response to changes of functional demands (Boonyarom & Inui, 2006; Flück, 2006) might occur during the habitat switches. For example, skeletal muscles increase in volume (hypertrophy) as a response to exercise and decrease their volume (atrophy) in response to immobility or extensive rest (Akima et al. 2000; Boonyarom & Inui, 2006; Kouzaki et al. 2007; Hanson et al. 2010). Accordingly, we aim to quantify potential changes in volume, fiber length and physiological cross-sectional area (PCSA) of the two main muscles powering suction feeding (M. rectus cervicis) and tongue protraction (M. subarcualis rectus). Given that under natural conditions suction feeding is the prevalent prey capture mode of the aquatic morphotype and tongue protraction the prevalent prey capture mode of the terrestrial morphotype in newts, we test whether Mm. subarcualis rectus and rectus cervicis hypertrophy/atrophy in a reciprocal manner as a response to changes in functional demands in the two morphotypes. Specifically, muscle hypertrophy of the M. rectus cervicis and atrophy of the M. subarcualis rectus in the aquatic morphotype and hypertrophy of the M. subarcualis rectus and atrophy of the M. rectus cervicis in the terrestrial morphotype were predicted.

Similar to muscle plasticity, different loading conditions on skeletal elements can cause structural changes (Matsuda et al. 1986; Lieberman et al. 2003). While in suction feeding, the elements of the hyobranchial skeleton act as a lever system to cause fast oropharyngeal volume expansion in a viscous medium, in lingual prehension the hyobranchial elements are slid in an anteroposterior direction to cause lingual pro- and retraction (Deban, 2003). As a consequence, suction feeding and lingual prehension pose different loading conditions on the hyobranchial skeleton. The last aim of this study is therefore to test for volumetric changes of representative skeletal elements across habitat shifts. Specifically, we predict increase in diameter and consequently higher volumes of the hyobranchial skeletal elements in the aquatic morphotypes where the hyobranchial skeleton forcefully pushes down on the floor of the oropharyngeal cavity for rapid volume expansion in a viscous med-

ium, which demands higher robustness of the skeletal elements compared with the sliding movements in tongue prehension.

Materials and methods

Fourteen adult Alpine newts (*I. alpestris*) and 14 adult smooth newts (*L. vulgaris*) were collected during their aquatic stage between May and June 2011 in Lower Austria, Austria with collection permission RU5-BE-18/022-2011 granted by the local government of Lower Austria. Animal husbandry and experiments were in strict accordance with national and international laws. Seven individuals for both species were immediately killed and fixed as described below to preserve their aquatic morphotype. The remaining animals were kept in a 150 L tank with water levels of 15 cm and an easily accessible land part. Food was offered both in water and on land, and animals were fed twice a week with a variety of red mosquito larvae (chironomids), firebrats (*Thermobia domestica*) and maggots (*Lucilia* sp.). Forty days after each individual newt had left the water and changed to the terrestrial habitat, it was anesthetized in 0.05% aqueous MS222 solution and killed by an intraperitoneal injection of Nembutal, cut in two pieces approximately 1 cm caudal to the shoulder girdle and immersed into fixation solution as described below. Individual mass was measured before death under anesthesia using a AS60 precision balance (Ohaus, Germany).

Histology

For histological analyses, two newts (all female) for each morphotype and species were immersed in Bouin's solution (Romeis, 1989; Kiernan, 2003) for 2 months, changing the solution every week. When decalcification was completed, samples were dehydrated in a graded ethanol-isopropanol series and embedded in paraffin. Next, 7- μ m serial-sections were made on a Reichert-Jung 2030 rotatory microtome (Reichert-Jung, Bensheim, Germany). The sections were mounted on glass slides and, after removing the paraffin, stained with Azan [see standard protocols after Romeis (1989) and Kiernan (2003)]. The preparations were documented by digital photography on a Nikon Eclipse E800 light microscope (Nikon, Tokyo, Japan).

Micro-computed tomography (μ CT)

For μ CT scanning, five newts (all male) for each morphotype and species were fixed in 4% formaldehyde for 1 month, changing the solution once a week. Then, specimens were dehydrated in a graded series of ethanol. In order to increase x-ray density of soft tissues, specimens were contrasted in a solution of 1% elemental iodine in absolute ethanol for 2 weeks (Metscher, 2009). After staining, samples were rinsed in absolute ethanol for several hours and mounted in Falcon tubes again in absolute ethanol. A scan of the whole head was acquired using a SkyScan 1174 (Bruker, Belgium) μ CT scanner with a source voltage of 50 kV and an isovolumetric voxel resolution of 7.39 μ m.

3D reconstruction

After image acquisition, image stacks were imported into the 3D software package AMIRA 4 (FEI Visualization Sciences Group, Merig-

nac Cedex, France). Based on tomographic image data, relevant structures were segmented either manually (cartilages, muscles) or by threshold segmentation (bones), and visualized via surface renderings. Volumes of the manually segmented muscles and skeletal elements of the hyobranchial apparatus were measured via Amira Material Statistics tool.

We measured the muscle volumes of two representative muscles with putative divergent functions in prey capture: M. rectus cervicis and m. subarcualis rectus. While the subarcualis rectus had a clear outline, the rectus cervicis is an extension of the rectus abdominis muscle of the ventral trunk musculature. Accordingly, given its 'blurry' and not always detectable origin (i.e. the first tendinous inscription) in μ CT scans, the anterior margin of the pericardium was defined as the posterior margin of the 'functional rectus cervicis'. This is justified with the fact that, according to previously published studies (Drüner, 1902; Francis, 1934; Özeti & Wake, 1969; Findeis & Bemis, 1990), the first tendinous inscription is located close to the anterior margin of the pericardium.

Determining fiber length and PCSA

To measure the mean muscle fiber length, all 20 individuals were dissected after μ CT scans were performed and individual muscles carefully removed. After dissection, muscles were immersed in 30% hydrous nitric acid solution to dissolve the collagenous tissue surrounding the muscle fibers (Nauwelaerts et al. 2007). After 24 h, muscles were rinsed in tap water for 5 min and immersed in a drop of 50% hydrous solution of glycerol on a glass slide. Muscle fibers were then carefully separated using two fine pins under a Karl Zeiss GSZ stereo microscope (Karl Zeiss, Jena, Germany) and covered with a coverslip (24 \times 60 mm). Next, digital micrographs were taken using an Olympus BX21 light microscope (Olympus, Japan), and the lengths of 20 randomly selected muscle fibers for each muscle were measured. The PCSAs of rectus cervicis and subarcualis rectus were calculated from muscle volume divided by mean fiber length (Maughan et al. 1983). Muscle volume was measured from the μ CT scans as described above.

Statistics

To quantify muscular changes, muscle volume and mean fiber lengths were bilaterally measured, and the PCSAs of the rectus cervicis and subarcualis rectus muscles were calculated in five individuals in both morphs of both species, resulting in a total of 80 measurements for each of the three factors. After positively testing for normal distribution of the residuals of the dependent variables, a multivariate analysis of covariance (MANCOVA) was performed, where muscle (rectus cervicis, subarcualis rectus), side (left, right), morphotype (aquatic, terrestrial) and species (*I. alpestris*, *L. vulgaris*) were treated as fixed factors; volume, fiber length and PCSA as dependent variables; and the individual's total body mass as co-factor. By entering the interaction effect of weight and morphotype into the MANCOVA, different effects (regression coefficient of body mass between morphotypes) of weight and morphotype were also modeled.

To quantify skeletal changes, the volumes of selected skeletal elements of the hyobranchial apparatus in both species were measured, namely the unpaired basibranchial, the ceratohyals (left and right) and the ceratobranchials 1 (left and right), resulting in a total of 100 measurements. Then, normal distribution of the residuals of the dependent variables was tested for. As the residuals were not

normally distributed, the data were log₁₀-transformed after which their residuals gained normal distribution. Next, an ANCOVA was performed, where skeletal element (basibranchial, ceratohyal and ceratobranchial 1), side (left, right, unpaired), morphotype (aquatic, terrestrial) and species (*I. alpestris*, *L. vulgaris*) were treated as fixed factors; volume as dependent variable; and the individual's total body mass as co-factor. By entering the interaction effect of weight and morphotype into the ANCOVA, different effects of weight and morphotype were modeled.

All statistical analyses were performed with Microsoft Excel 2010 and SPSS Statistics 20 software package.

Results

The architecture of the cranio-cervical musculoskeletal system

Qualitative differences between aquatic and terrestrial stages were not obvious and differences between species were marginal, though the heads in *I. alpestris* appeared to be broader compared with *L. vulgaris* (compare Fig. 1 with Fig. 2). Accordingly, the generalized morphology is described below. Description and terminology largely follows Drüner (1902, 1904), Francis (1934), Özeti & Wake (1969) and Findeis & Bemis (1990).

The skeletal system

The skull. The upper jaw consists of the premaxilla and the maxilla (Figs 1A,B and 2A,B), both of which bear teeth. Dorsally, behind the premaxilla lie the paired nasals, frontals and parietals that together build up the roof of the braincase (Figs 1A,B and 2A,B). Posterior to the parietals lie the exoccipitals, which enclose the braincase posteriorly. The exoccipitals also bear the exoccipital condyles that articulate with the atlas (Figs 1A–C and 2A–C). The floor of the braincase is built up by the paired vomers anteriorly and the large unpaired parasphenoid posteriorly (Figs 1B,C and 2B,C). The vomers bear a longitudinally arranged row of teeth that overlap the parasphenoid that is connected posteriorly to the exoccipitals. The pterygoids have a broad base on the ventral exoccipital as well as on the medial squamosal and extend anteroventrally with their elongated process (Figs 1B and 2B). The squamosal is connected laterally on the skull, between the parietal and the exoccipital bones and bears on its distal side the quadrate, which articulates with the articular of the mandible (Figs 1B and 2B). The articular is attached anteriorly on the tooth bearing dentary (Figs 1B and 2B).

The hyolingual system. The hyolingual system in both newt species mainly lies between the mandibular rami and extends up to the posterior pharynx (Figs 1B–D and 2B–D). The unpaired bony basibranchial lies centrally in the floor of the mouth and forms the main axis of the hyolingual

apparatus (Figs 1B–D and 2B–D). The very anterior tip of the basibranchial is cartilaginous and articulates with the paired radii, which are connected through a cartilaginous bow, the interradii cartilage (Figs 1D and 2D). Posteriorly, the unpaired basibranchial element articulates with the first and second hypobranchials (Figs 1C,D and 2C,D). The first hypobranchials are thick, bony and articulate posteriorly with the first ceratobranchials, which are also bony in nature (Figs 1B–D and 2B–D). The second hypobranchials are slender and cartilaginous, and their posterior end attaches to the articulation of the first hypobranchial and the first ceratobranchial (Figs 1C,D and 2C,D). The ceratohyals lie medial to the mandibular rami and consist of a cartilaginous spade-like-shaped anterior part and a bony posterior part that is posterodorsally flexed and becomes gradually roundish towards its posterior end (Figs 1B–D and 2B–D).

The muscular system

Epaxial musculature. The epaxial musculature in both *I. alpestris* and *L. vulgaris* insert on the posterior skull by three main portions: the dorsal-most portion forms the bulk of the epaxial musculature and is represented by the M. dorsalis trunci that attaches to the posterior exoccipital and squamosal (Figs 1A',B' and 2A',B'). Beneath the M. dorsalis trunci lies the relatively slender M. intertransversarius capitis superior that attaches beneath the M. dorsalis trunci on the exoccipital and squamosal (Fig. 3F). The third main portion of the anterior epaxial musculature is represented by the M. intertransversarius capitis inferior that runs beneath both Mm. dorsalis trunci and intertransversarius capitis superior to insert on the ventral exoccipital region (Figs 1B', 2B' and 3F), beneath the articulation of skull and atlas.

Jaw muscles. The jaw muscles consist of the jaw depressor and the jaw adductor systems. The jaw depressor system is represented by the M. depressor mandibulae that originates on the posterior squamosal and runs ventrally to insert on the articular, posterior to the jaw joint (Figs 1A',B', 2A',B' and 3E). The jaw adductor system is represented by the M. adductor mandibulae complex that is composed of several portions. The M. adductor mandibulae internus can be subdivided into a superficial and a deep portion (Figs 1A',B', 2A',B' and 3D). The superficial portion originates on the spinal process of the first vertebra and on the fasciae of the epaxial musculature and runs antero-ventrally to insert on the articular bone anterior to the jaw joint (Figs 1A',B', 2A',B' and 3D). The deep portion has a broader origin, extending from the frontal to the parietal and runs ventrally to insert on the articular, anterior to the jaw joint (Figs 1A',B', 2A',B' and 3D). The M. adductor mandibulae externus originates on the anterior proximal squamosal, follows the squamosal ventrally and inserts on the articular, anterior to the jaw joint (Figs 1A',B', 2A',B' and 3D).

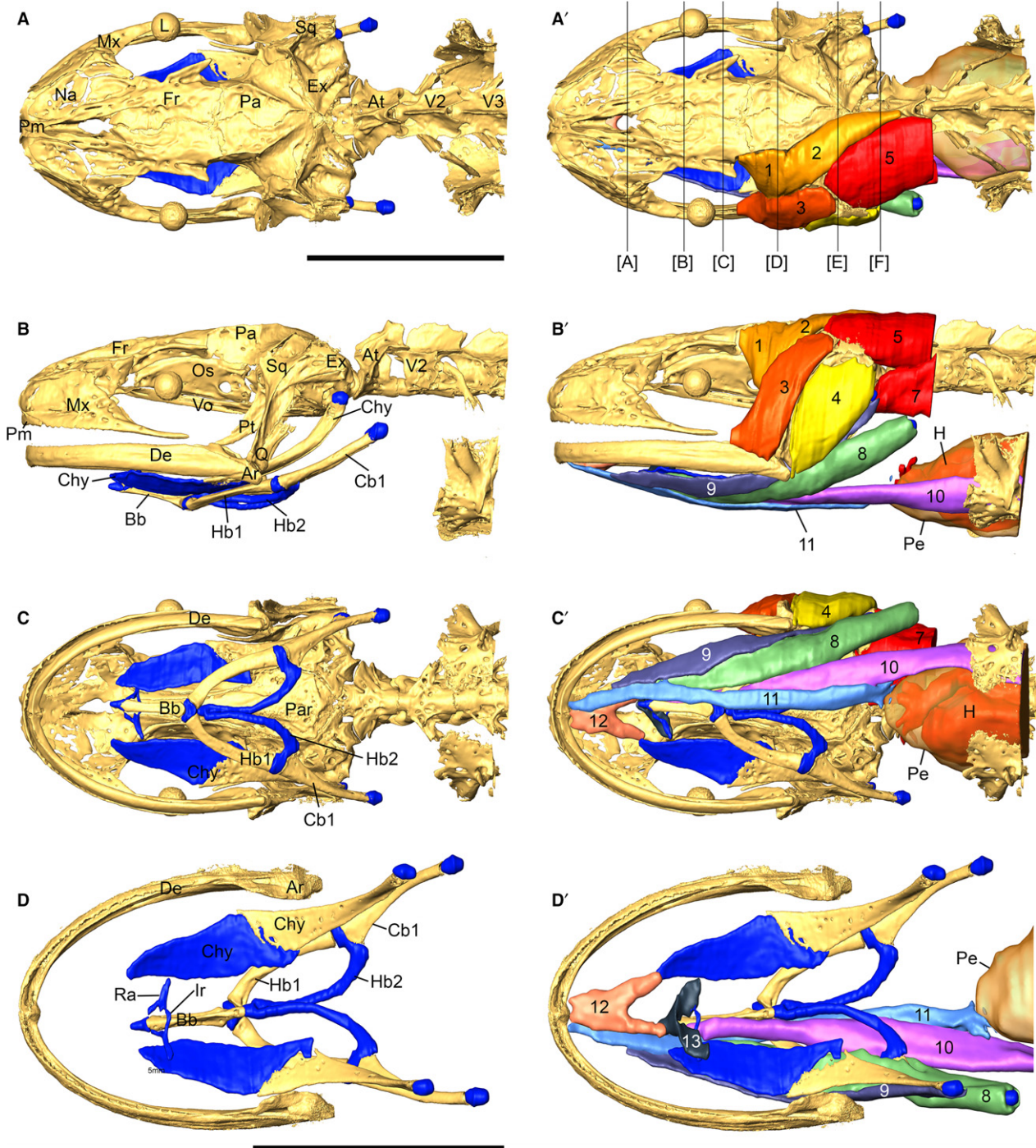


Fig. 1 3D reconstructions of the skeletal (A–D) and the corresponding musculoskeletal (A'–D') architecture of the cranio-cervical system in *Lissotriton vulgaris* from dorsal (A, A'), lateral (B, B') and ventral views (C, C'). D and D' show the hyobranchial apparatus from dorsal view after virtual removal of the skull. Abbreviations: (i) Skeletal elements: Ar, articular; At, atlas; Bb, basibranchial; Cb1, ceratobranchial 1; Chy, ceratohyal; De, dentary; Ex, exoccipital; Fr, frontal; Hb1, hypobranchial 1; Hb2, hypobranchial 2; Ir, interradial cartilage; Mx, maxillary; Na, nasal; Os, orbitosphenoid; Pa, parietal; Par, parasphenoid; Pm, premaxillary; Pt, pterygoid; Q, quadrate; Ra, radial; Sg, shoulder girdle; Sq, squamosal; V2, second vertebra; V3, third vertebra; Vo, vomer. (ii) Muscles: 1, adductor mandibulae internus (deep portion); 2, adductor mandibulae internus (superficial portion); 3, adductor mandibulae externus; 4, depressor mandibulae; 5, dorsalis trunci; 7, intertransversarius capitis inferior; 8, subarcualis rectus; 9, subhyoideus; 10, rectus cervicis (both superficialis and profundus); 11, geniopharyngeus; 12, genioglossus; 13, basiradialis. (iii) Other structures: L, lens; Pe, pericardium. Scale bars: 5 mm. The vertical lines in A' indicate the area of the histological cross-sections shown in Fig. 3.

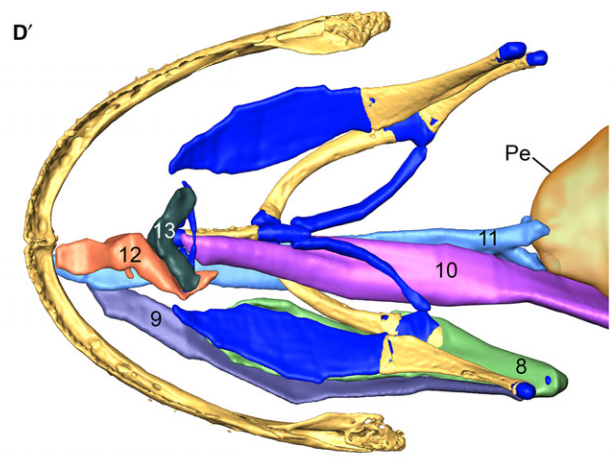
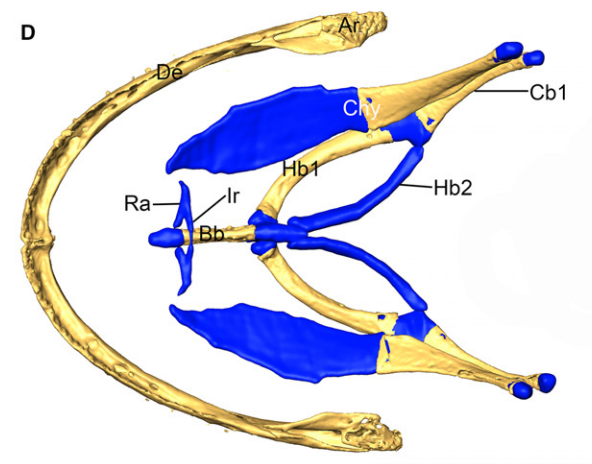
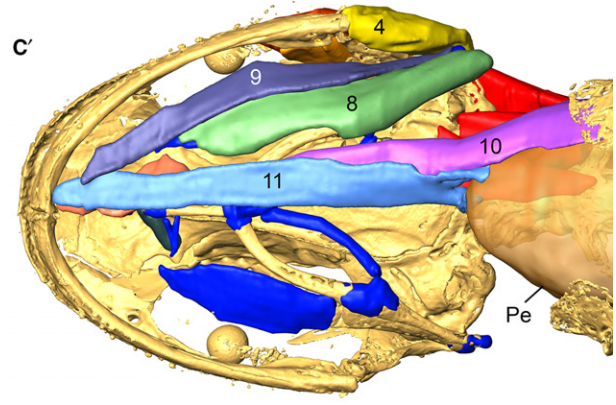
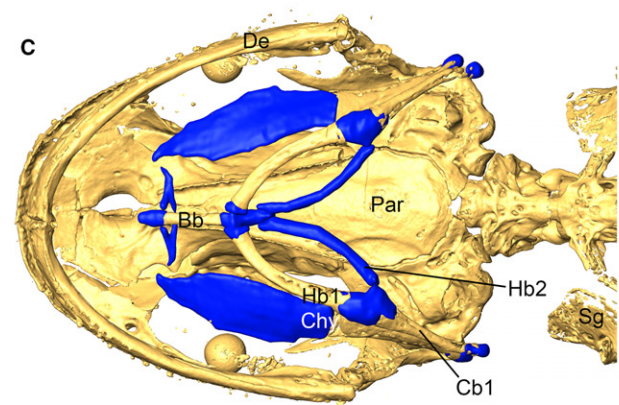
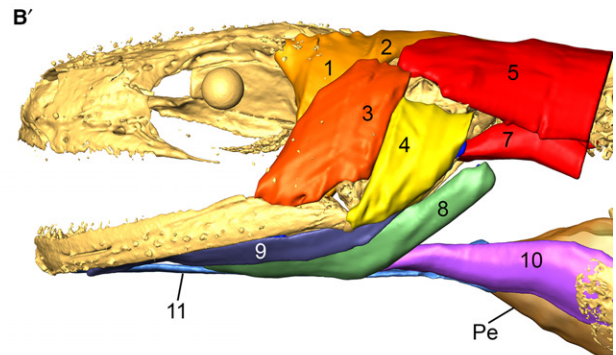
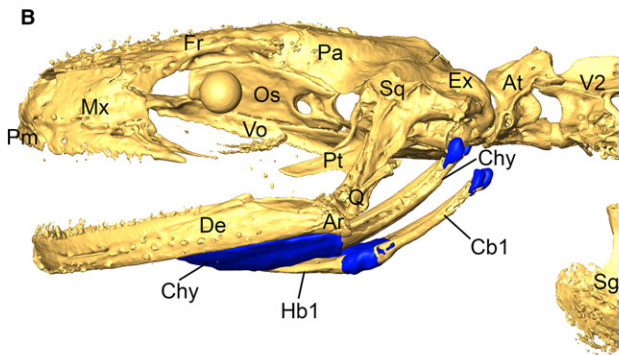
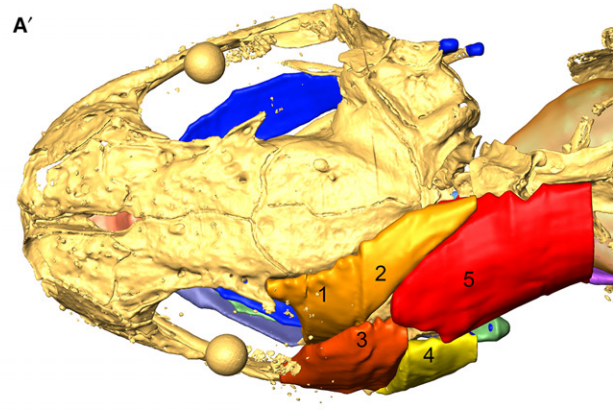
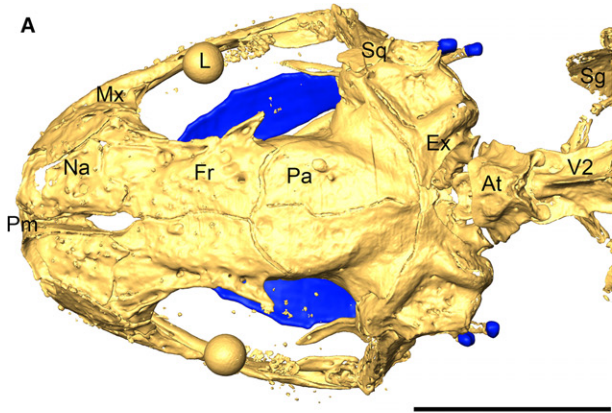


Fig. 2 3D architecture of the skeletal (A–D) and the corresponding musculoskeletal (A'–D') cranio-cervical system in *Ichthyosaura alpestris* from dorsal (A, A'), lateral (B, B') and ventral views (C, C'). D and D' show the hyobranchial apparatus from dorsal view after virtual removal of the skull. Abbreviations: (i) Skeletal elements: Ar, articular; At, atlas; Bb, basibranchial; Cb1, ceratobranchial 1; Chy, ceratohyal; De, dentary; Ex, exoccipital; Fr, frontal; Hb1, hypobranchial 1; Hb2, hypobranchial 2; Ir, interradial cartilage; Mx, maxillary; Na, nasal; Os, orbitosphenoid; Pa, parietal; Par, parasphenoid; Pm, premaxillary; Pt, pterygoid; Q, quadrate; Ra, radial; Sg, shoulder girdle; Sq, squamosal; V2, second vertebra; Vo, vomer. (ii) Muscles: 1, adductor mandibulae internus (deep portion); 2, adductor mandibulae internus (superficial portion); 3, adductor mandibulae externus; 4, depressor mandibulae; 5, dorsalis trunci; 7, intertransversarius capitis inferior; 8, subarcualis rectus; 9, subhyoideus; 10, rectus cervicis (both superficialis and profundus); 11, geniohyoideus; 12, genioglossus; 13, basiradialis. (iii) Other structures: H, heart; L, lens; Pe, pericardium.

Muscles of the hyoid (throat) region. Three main hyoid muscles were distinguished in *I. alpestris* and *L. vulgaris*. Anteriorly, the M. intermandibularis posterior originates medially on the dentaries, runs transversely and both contralateral parts are connected by the median aponeurosis, which accordingly represents the insertion site (Fig. 3A–C). The M. intermandibularis posterior overlaps more posteriorly with the interossea quadrata muscle. The M. interossea quadrata originates on a cartilage between proximal quadrate bone and pterygoid and runs transversally where it becomes significantly broader towards its insertion site, the median aponeurosis (Fig. 3D,E). The interhyoideus posterior originates from the posterior quadrate and distal posterior squamosal and runs in a postero-ventral direction to broadly insert on the pectoral girdle (not shown).

Tongue- and hyobranchial musculature. The muscles of the tongue and the hyobranchial system are responsible for the complex movements of the hyobranchial elements relative to each other and the hyobranchial apparatus relative to the lower jaw. The M. genioglossus originates on the dentary, close to the mandibular symphysis, and its fibers fan out into the tongue pad and the floor of the mouth where the fibers diffusely insert on the mucosa (Figs 1D', 2D' and 3A). The M. geniohyoideus attaches together with the M. genioglossus lateral to the mandibular symphysis (Figs 1C',D' and 2C',D') on the dentary and runs caudally, just above the slender superficial throat muscles (Fig. 3A–E). Most of the geniohyoideus fibers originate on the anterior pericardium (Figs 1C',D', 2C',D', 3F, 4F and 5). The M. subhyoideus muscle originates on the posterior end of the ceratohyal, follows its shaft ventrally and laterally up to the very anterior floor of the mouth to insert on the fasciae between Mm. geniohyoideus and intermandibularis posterior (Figs 1C',D', 2C',D', 3A–E and 4A–E). The M. subarcualis rectus originates on the posterior portion of the first ceratobranchial (Figs 1B'–D', 2B'–D', 3B–F and 4B–F). Its fibers run anteriorly, following the course of first ceratobranchial and first hypobranchial by literally enwrapping them and finally inserts on the ventral surface of the anterior portion of the ceratohyal (Figs 1B'–D', 2B'–D', 3B–F and 4B–F). The rectus cervicis system is a direct continuation of the rectus abdominis muscle but separated from it by the first tendinous inscription that represents its origin. The superficial portion, the M. rectus cervicis superficialis, is thin and extends anteri-

orly to insert on the posterior-most part of the basibranchial where the first ceratobranchial attaches to the basibranchial bone (Figs 1B'–D', 2B'–D', 3D–F and 4D–F). The deeper portion, the M. rectus cervicis profundus, represents the main body of the rectus cervicis muscle. From its origin (the first tendinous inscription) its fibers run anteriorly, above (i.e. dorsally) along the M. rectus cervicis superficialis, and insert both on the anterior-most basibranchial and the interradial cartilage that connects left and right radii (Figs 1B'–D', 2B'–D', 3B–F and 4B–F). Anterior to the radii lies the basiradialis muscle that originates on the anterior basibranchial to run posteriorly and inserts on the anterior faces of the radii (Figs 1D', 2D', 3A and 4A).

Quantitative changes of the hyobranchial myoskeletal system across morphotypes

Descriptive statistics of muscle volumes, PCSAs and fiber lengths are shown in Table 1. The MANCOVA designed to test for muscle volume, fiber length and PCSA differences across muscle, side, morphotype and species yielded significant differences between morphotypes (Wilks' lambda $F_{3,60} = 3.766$, $P = 0.015$) and muscle (Wilks' lambda $F_{3,60} = 21.32$, $P < 0.001$), but no significant differences between side (Wilks' lambda $F_{3,61} = 0.03$, $P = 0.99$) and species (Wilks' lambda $F_{3,60} = 0.68$, $P = 0.57$). Because of a significant interaction effect between species and morphotypes (Wilks' lambda $F_{3,60} = 7.26$, $P < 0.001$), subsequent *post hoc* tests were performed for morphotypes for both species with Bonferroni correction. Pairwise comparison revealed significant differences between muscle volume in the two morphotypes in *L. vulgaris* ($P = 0.023$) and *I. alpestris* ($P = 0.027$), between PCSA in the two morphotypes in *L. vulgaris* ($P = 0.001$) and *I. alpestris* ($P = 0.009$), but no significant differences between fiber length in the two morphotypes in both species. The significant interaction effect between species and morphotypes in the MANCOVA was based on the fact that values for PCSA and muscle volume were higher in the terrestrial compared with the aquatic morphotype in *L. vulgaris*, but reversely higher in the aquatic compared with the terrestrial morphotype in *I. alpestris* as evidenced by the values of the estimated marginal means.

Descriptive statistics of hyobranchial skeletal element volumes are shown in Table 2. The ANCOVA designed to test for volumetric differences of the hyobranchial skeletal ele-

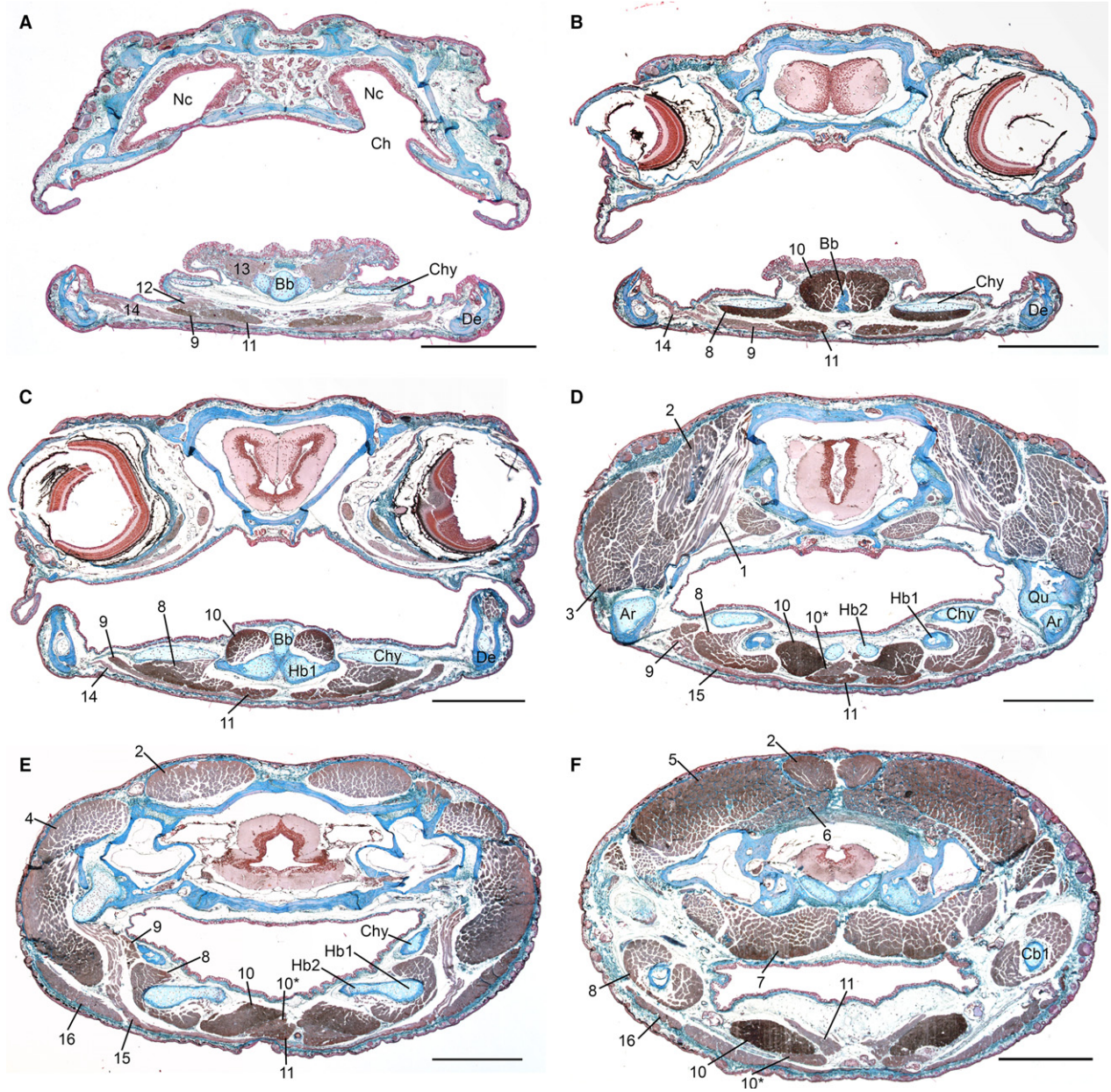


Fig. 3 Light micrographs of histological cross-sections through the head of *Lissotriton vulgaris* in its aquatic stage. For a better orientation, vertical lines in Fig. 1A' indicate the regions of the sections. Abbreviations: Ar, articular; Bb, basibranchial; Cb1, ceratobranchial 1; Ch, choana; Chy, ceratohyal; Hb1, hypobranchial 1; Hb2, hypobranchial 2; Nc, nasal cavity; Q, quadrate. Muscles: 1, adductor mandibulae internus (deep portion); 2, adductor mandibulae internus (superficial portion); 3, adductor mandibulae externus; 4, depressor mandibulae; 5, dorsalis trunci; 6, intertransversarius capitis superior; 7, intertransversarius capitis inferior; 8, subarcualis rectus; 9, subhyoideus; 10, rectus cervicis profundus; 10*, rectus cervicis superficialis; 11, geniohyoideus; 12, genioglossus; 13, basiradialis; 14, intermandibularis posterior; 15, interossa quadrata; 16, interhyoideus posterior (the numbering of the muscles corresponds with Fig. 1 where appropriate). Azan staining; scale bars: 1 mm.

ments revealed highly significant differences between the three elements ($F_{1,78} = 139.92$; $P < 0.001$), but no differences between sides ($F_{1,78} = 0.003$; $P = 0.96$), morphotypes ($F_{1,78} = 1.183$; $P = 0.28$) or species ($F_{1,78} = 0.005$; $P = 0.941$). Because of a significant interaction effect between species and morphotype ($F_{1,78} = 8.571$; $P = 0.004$), subsequent *post hoc* tests were performed for morphotypes for both species with

Bonferroni correction. Pairwise comparison revealed significant differences between skeletal element volumes in the two morphotypes in *L. vulgaris* ($P = 0.027$) and *I. alpestris* ($P = 0.027$). The significant interaction effect between species and morphotypes in the ANCOVA was based on the fact that values for volume were higher in the terrestrial compared with the aquatic morphotype in *L. vulgaris*, but rever-

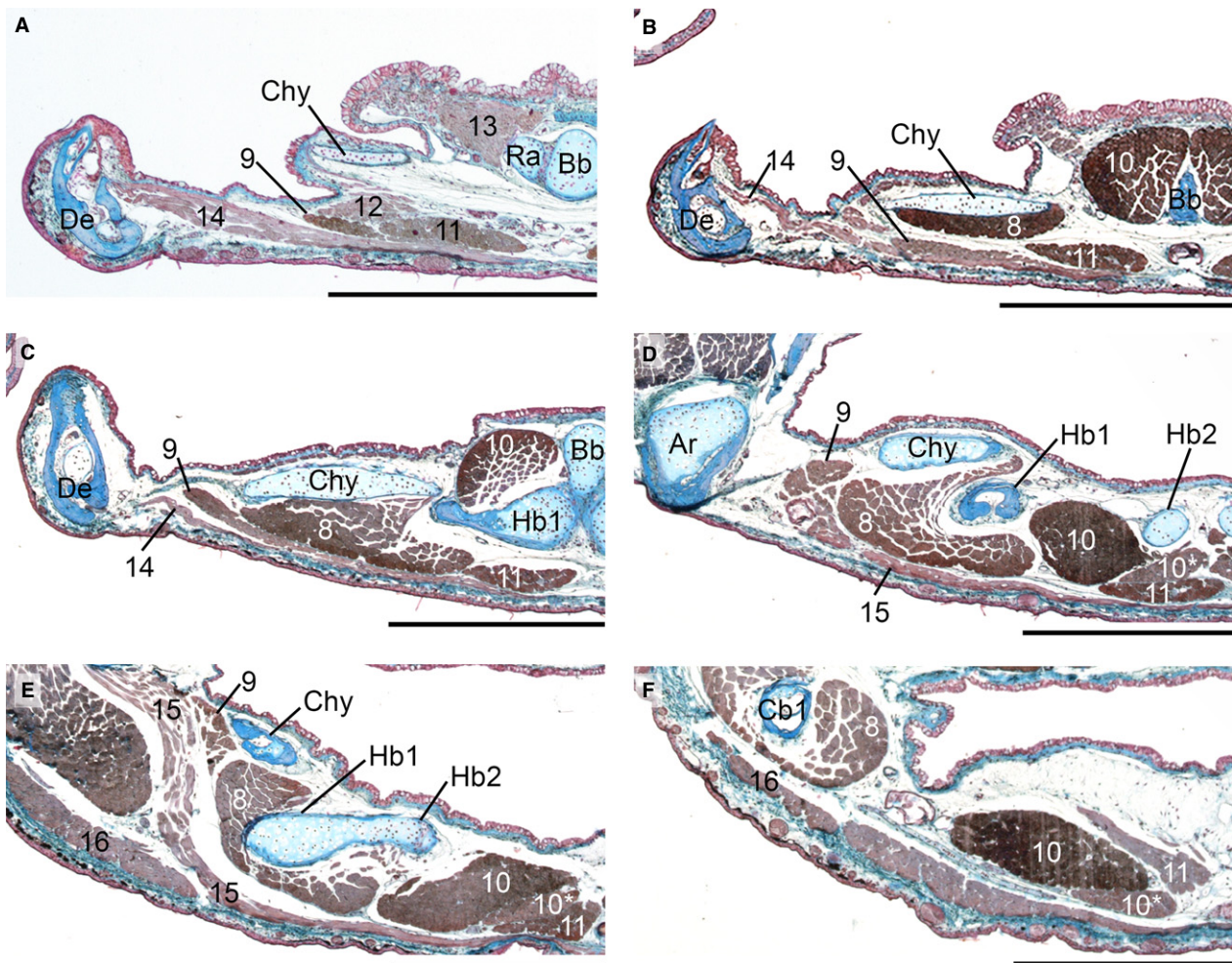


Fig. 4 More detailed views of the micrographs in Fig. 3, showing in detail elements of the right hyobranchial musculoskeletal system in *Lissotriton vulgaris*. Abbreviations: Ar, articular; Bb, basibranchial; Cb1, ceratobranchial 1; Chy, ceratohyal; De, dentary; Hb1, hypobranchial 1; Hb2, hypobranchial 2; Ra, radial. Muscles: 8, subarcualis rectus; 9, subhyoideus; 10, rectus cervicis profundus; 10*, rectus cervicis superficialis; 11, geniopharyngeus; 12, genioglossus; 13, basiradialis; 14, intermandibularis posterior; 15, interossea quadrata; 16, interhyoideus posterior. Azan staining; scale bars: 1 mm.

sely higher in the aquatic compared with the terrestrial morphotype in *I. alpestris* as evidenced by the estimated marginal means.

Discussion

Form and function of the feeding apparatus

The newt species *I. alpestris* and *L. vulgaris* exhibit seasonal habitat changes and typically use one of two different prey capture strategies, namely suction feeding in the aquatic stage and tongue prehension in the terrestrial stage (Heiss et al. 2013, 2015). Suction feeding and tongue prehension are conflicting functions as both strategies place different demands on the prey capture apparatus (Deban, 2003). Newts belong to the very few (if not only) vertebrates that can use both strategies in an effective way. Accordingly,

they are faced with different demands on the musculoskeletal system to effectively capture prey in both environments.

So how does the musculoskeletal system operate to perform the different functions successfully? The exact muscle functions are not known yet but can be predicted based on their line-of-action. Accordingly, the function of the prey capture apparatus is reconstructed based on previously published work (Drüner, 1902, 1904; Francis, 1934; Özeti & Wake, 1969; Lauder & Reilly, 1988, 1994; Findeis & Bemis, 1990; Reilly & Lauder, 1992; Deban & Wake, 2000; Wake & Deban, 2000; Deban, 2003) and the anatomical descriptions of the present study. For aquatic prey capture, newts use fast opening of the jaws, followed by hyobranchial depression. Jaw opening is achieved first by ventral rotation of the lower jaw, presumably driven by action of the M. depressor mandibulae and second by dorsal rotation of the skull by

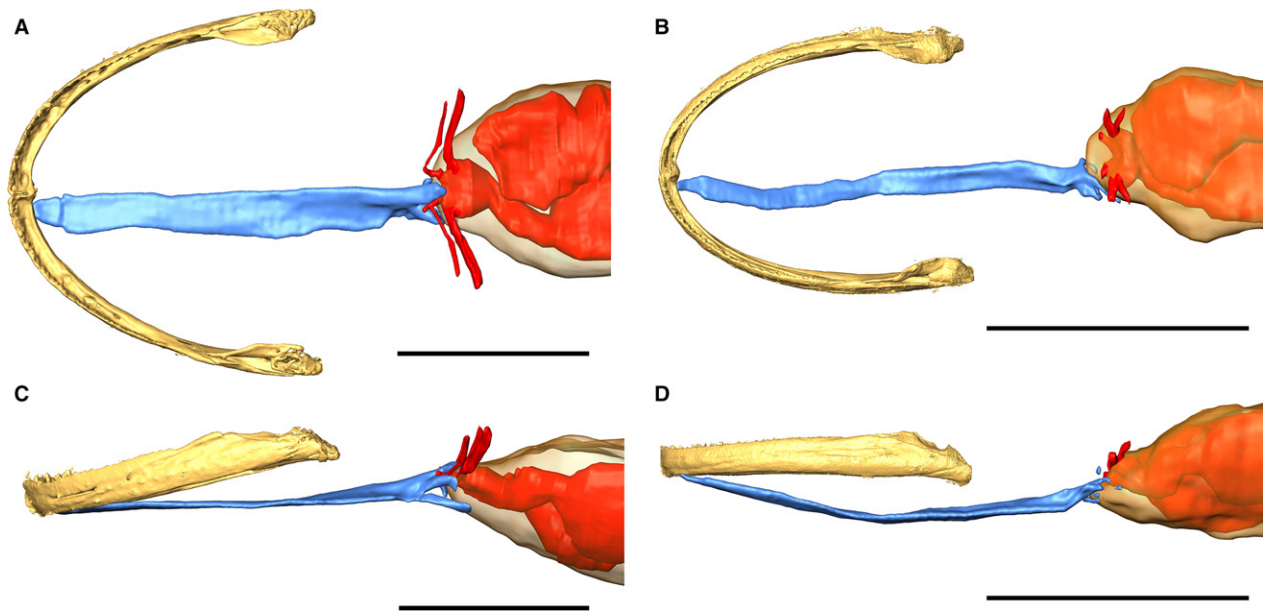


Fig. 5 3D reconstructions showing the special arrangement of the geniohyoideus muscle that connects the lower jaw with the pericardium in *Ichthyosaura alpestris* (A, C) and *Lissotriton vulgaris* (B, D). All structures except lower jaw, geniohyoideus, pericardium and heart were virtually removed. A and B: dorsal views; C and D, lateral views. Scale bars: 5 mm.

Table 1 Descriptive statistics of rectus cervicis and subarcualis rectus muscle volume, fiber length and PCSA in the two newt species *Ichthyosaura alpestris* and *Lissotriton vulgaris* with two distinct morphotypes.

Species	Morphotype	Muscle	Mean volume \pm SE (mm ³)	Mean fiber length \pm SE (mm)	PCSA \pm SE (mm ²)
<i>I. alpestris</i>	Aquatic	Rectus cervicis	2.71 \pm 0.31	5.55 \pm 0.08	0.49 \pm 0.05
		Subarcualis rectus	2.63 \pm 0.31	4.7 \pm 0.17	0.55 \pm 0.05
	Terrestrial	Rectus cervicis	2.48 \pm 0.25	5.72 \pm 0.26	0.43 \pm 0.03
		Subarcualis rectus	2.45 \pm 0.28	5.05 \pm 0.24	0.47 \pm 0.04
<i>L. vulgaris</i>	Aquatic	Rectus cervicis	1.61 \pm 0.16	5.51 \pm 0.2	0.29 \pm 0.02
		Subarcualis rectus	1.83 \pm 0.21	4.78 \pm 0.15	0.37 \pm 0.03
	Terrestrial	Rectus cervicis	1.91 \pm 0.20	5.57 \pm 0.1	0.35 \pm 0.03
		Subarcualis rectus	2.15 \pm 0.26	4.95 \pm 0.14	0.43 \pm 0.04

PCSA, physiological cross-sectional area.

contraction of the M. dorsalis trunci and M. intertransversarius capitis superior (epaxial muscles). Mouth closure is achieved by dorsal rotation of the lower jaw through the adductor mandibulae complex and ventral rotation of the skull by contraction of the M. intertransversarius capitis inferior of the epaxial musculature that inserts on the exoccipital, ventral to the articulation of the skull with the atlas. Posteroventral rotation of the hyobranchial system is achieved by action of the rectus cervicis system and stabilized by a set of smaller muscles and ligaments that were not shown in this study. Contraction of the genioglossus muscle, together with the transversally running intermandibularis posterior and interossa quadrata might bring the hyobranchial system to its resting position. For terrestrial feeding in the aquatic stage, both *I. alpestris* and *L. vulgaris* use jaw prehension (Heiss et al. 2013, 2015). The

movement patterns of jaw prehension and suction feeding are very similar and, accordingly, the same set of muscles might be involved in driving jaw and hyobranchial movements in jaw prehension with slightly modified activation patterns. However, jaw and hyobranchial movement patterns for terrestrial feeding change significantly when newts change to their terrestrial stage. In their terrestrial stage, newts use tongue prehension to capture prey that requires different, well-coordinated movement patterns and presumably muscle functions. Mouth opening and closing are achieved as described above, though the kinematic gape profile in the tongue prehension mode (two peaks) shows distinct differences to the suction feeding- and the jaw prehension mode (one peak; Heiss et al. 2013, 2015). Protraction of the tongue is presumably achieved by complex interplay of several musculoskeletal elements. First,

Table 2 Descriptive statistics of basibranchial, ceratobranchial 1 and ceratohyal volume in *Ichthyosaura alpestris* and *Lissotriton vulgaris* with two distinct morphotypes.

Species	Morphotype	Skeletal element	Mean volume \pm SE (mm ³)
<i>I. alpestris</i>	Aquatic	Basibranchial	0.35 \pm 0.06
		Ceratobranchial 1	0.41 \pm 0.05
		Ceratohyal	1.04 \pm 0.13
	Terrestrial	Basibranchial	0.26 \pm 0.04
		Ceratobranchial 1	0.36 \pm 0.02
		Ceratohyal	1.02 \pm 0.04
<i>L. vulgaris</i>	Aquatic	Basibranchial	0.22 \pm 0.04
		Ceratobranchial 1	0.36 \pm 0.04
		Ceratohyal	0.77 \pm 0.12
	Terrestrial	Basibranchial	0.24 \pm 0.04
		Ceratobranchial 1	0.36 \pm 0.05
		Ceratohyal	0.9 \pm 0.09

contraction of the subhyoideus muscle moves the whole hyobranchial system forwards. This movement might be assisted by contraction of the genioglossus muscle, which fans from its origin site on the lower jaw into the tongue. Next, the ceratohyals act as anchor structures and contraction of the M. subarcualis rectus, which runs from the posterior tip of the ceratobranchial 1 to the anterior ceratohyal, pulls the brachial system anteriorly, relative to the ceratohyals. During tongue protraction, the tongue pad is flipped anteroventrally by contraction of the basiradialis muscle that runs between the anterior-most basibranchial and the anterior face of the interradial cartilages. Retraction of the whole hyobranchial system is finally achieved by contraction of the rectus cervicis system. Elevation of the throat by action of the transversally running muscles intermandibularis posterior and interossa quadrata brings the whole hyobranchial system back to its resting position (Deban, 2003).

The special case of the M. geniohyoideus in newts

The geniohyoideus muscle is one of the main hyobranchial muscles in virtually all tetrapods and ancestrally connects the hyobranchial skeletal system with the lower jaw (Deban & Wake, 2000; Hiemae, 2000; Nishikawa, 2000; O'Reilly, 2000; Schwenk, 2000a,b; Wake & Deban, 2000; Heiss et al. 2011). Accordingly, its function is associated with lower jaw depression (when the hyobranchium is fixed by action of rectus cervicis/sternohyoideus muscle) and hyobranchial protraction (with relaxed rectus cervicis/sternohyoideus). However, in metamorphosed newts, though the M. geniohyoideus insertion on the lower jaw remains in place, its origin and accordingly its course differ substantially from other tetrapods. In salamander larvae, the M. geniohyoideus runs from the lower jaw posteriorly and attaches on the urohyal: the posterior-most hyobranchial skeletal element that is attached to the rest of the hyobranchial system

(Drüner, 1902; Reilly, 1987; Reilly & Lauder, 1990; Deban & Wake, 2000; Kleinteich et al. 2014). During metamorphosis in salamandrids, the urohyal loses its connection with the hyobranchial system or is completely lost in some salamandrids (Francis, 1934) along with the origin of the M. geniohyoideus. As already shown by Drüner (1902) and Özeti & Wake (1969) in several salamandrids, as well as Francis (1934) in the fire salamander, though most of the geniohyoideus fibers originate on the 'os triangularis' (i.e. the rest of the urohyal) or the first tendinous inscription, some of its lateral fibers originate on the 'capsule of the thyroid gland' (Francis, 1934), just anterior to the pericardium. As shown by Findeis & Bemis (1990) in *Taricha torosa* and in this study in *I. alpestris* and *L. vulgaris*, after reduction of its primary origin (the urohyal) during metamorphosis, the M. geniohyoideus originates on the anterior pericardium and only few fibers attach to the first tendinous inscription. Interpreting the function of a muscle that basically connects the lower jaw with the pericardium might be problematic at first sight. Findeis & Bemis (1990) hypothesized that contraction of the geniohyoideus muscle assists action of the M. depressor mandibulae in depressing the lower jaw. When the adductor system would be activated at the same time, however, Francis (1934) hypothesized that contraction of the geniohyoideus might pull the pericardium with the heart and associated structures anteriorly. To the authors' current knowledge the latter function seems unlikely. However, given that the pericardium in *I. alpestris* and *L. vulgaris* is embedded in the hypaxial musculature between the shoulder girdles, it might well be that the pericardium is fixed in its position and mechanically stable enough to allow contraction of the geniohyoideus in assisting throat elevation (with activated adductor system) and lower jaw depression (with relaxed adductor system). Future integrative experimental approaches, such as combined kinematic and electromyographic studies, are needed to unravel the function of the extraordinary geniohyoideus muscle in newts.

Do seasonal habitat shifts induce quantitative changes of the hyobranchial musculoskeletal system?

Skeletal muscles in vertebrates respond with structural plasticity to changing functional demands (Boonyarom & Inui, 2006; Flück, 2006). For example, many studies have shown that exercise induces skeletal muscle growth, which is mainly achieved by an increase of individual myofiber size (Goldberg et al. 1974; Lüthi et al. 1986; Boonyarom & Inui, 2006; Folland & Williams, 2007). In seasonally habitat-changing newts, aquatic and terrestrial morphotypes rely on different prey capture strategies that are powered by different muscles. Specifically, the rectus cervicis system is the main muscle system powering fast posteroventral rotation of the hyobranchial elements that is used for suction feeding, while the subarcualis rectus system accelerates the

tongue out of the mouth for tongue prehension (Özeti & Wake, 1969; Larsen & Guthrie, 1975; Findeis & Bemis, 1990; Wake & Deban, 2000; Deban, 2003). Accordingly, it was hypothesized that volume and PCSA values of rectus cervicis and subarcualis rectus change across habitat shifts as response to the changed functional demands. Specifically, a reciprocal scenario was expected: muscle hypertrophy of the rectus cervicis and atrophy of the subarcualis rectus in the aquatic morphotype and hypertrophy of the subarcualis rectus and atrophy of the rectus cervicis in the terrestrial morphotype. Similarly, suction feeding and lingual prehension pose different loading conditions on the hyobranchial skeleton, and volumetric changes of representative skeletal elements across habitat shifts and, consequently, morphotypes were expected.

The hypothesised pattern was not found in the current study. Both muscle volumes and PCSAs of rectus cervicis and subarcualis rectus as well as the volumes of the hyobranchial skeletal elements were significantly higher in the terrestrial compared with the aquatic morphotype in *L. vulgaris*. Conversely, in *I. alpestris*, muscle volumes, PCSAs and the volumes of the hyobranchial skeletal elements were significantly higher in the aquatic compared with the terrestrial morphotype. Accordingly, the changes of the hyobranchial system across morphotypes in the seasonally habitat changing newts were different as predicted. A similar pattern of quantitative morphological changes was expected in both species based on diverging functional demands in aquatic and terrestrial morphotypes, but all tested musculoskeletal hyobranchial elements hypertrophied in the terrestrial morphotype in *L. vulgaris* but hypertrophied in the aquatic morphotype in *I. alpestris* and no evidence for a function-based reciprocal change was evident. If a reciprocal change would have been the case, the rectus cervicis muscle and the hyobranchial skeletal elements should have hypertrophied in the aquatic morphotype and, at the same time, the subarcualis rectus should have hypertrophied in the terrestrial morphotype in both species.

So, why isn't there a general pattern of hypertrophy/atrophy in both newt species and why do newts not reciprocally hypertrophy/atrophy the rectus cervicis and subarcualis rectus muscle systems despite different functional demands between prey capture on land and in water? The present study raises these questions but will not be able to finally untangle them. However, a possible answer to the first question could be that both newt species are not equally well adapted to both aquatic and terrestrial lifestyles, and that the whole prey capture apparatus might show hypertrophy in the prevalent aquatic (*I. alpestris*) or terrestrial (*L. vulgaris*) lifestyle. In other words, *I. alpestris* might feed more frequently in the aquatic stage, but *L. vulgaris* in the terrestrial stage, and hence they gain overall cranial muscle through exercise in different stages. To tackle the second question why there are no reciprocal changes of the muscular system across morphotypes, it might be argued that

both muscle systems are active during both feeding strategies despite performing different functions. For example, the rectus cervicis, besides powering suction feeding in the aquatic morphotype, is also responsible for tongue retraction in the terrestrial morphotype. Similarly, former studies on ambystomatid salamanders have shown that the subarcualis rectus is activated during the initial phase of suction feeding (Lauder & Shaffer, 1988). Accordingly, one interpretation of the current results is that though functional demands change between aquatic and terrestrial morphotypes in newts, this only results in small changes of the neuromotor recruitment and consequently in the muscle activity pattern. This means that even a small change in the muscle activity pattern that involves the same set of cranial muscles can result in two very different functions, namely suction feeding and tongue prehension (Shaffer & Lauder, 1988). In other words, despite the changing demands on maximal power production between muscle groups in one of the two feeding modes, all main cranial muscles are active in both feeding modes and this might circumvent reciprocal muscle hypertrophy/atrophy when newts switch habitat. However, muscle plasticity does not exclusively rely on muscle volume or PCSA changes, and other factors, such as changes in the capillary network and supply area of the muscles, changes in myofibril ultrastructure or molecular mechanisms (Boonyarom & Inui, 2006; Flück, 2006; Gerth et al. 2009) may be considered in future studies.

Acknowledgements

The authors thank Günter Schultschik for important information on the ecological background of newts and for providing advice on collection sites and husbandry of newts; the local government of Lower Austria for granting the animal collection permission; Christian Proy, Monika Lintner, Marion Hüffel and Thomas Pecina for their enthusiastic help in collecting newts; Monika Lintner for assistance in histology; Brian Metscher for performing the μ CT scans; Alexander Rabanser for statistical advice; and Nicolai Konow along with two anonymous reviewers for helpful comments on the manuscript. This study was supported by the Austrian Science Fund FWF (J3186-B17).

References

- Akima H, Kawakami Y, Kubo K, et al. (2000) Effect of short-duration spaceflight on thigh and leg muscle volume. *Med Sci Sports Exerc* **32**, 1743–1747.
- Boonyarom O, Inui K (2006) Atrophy and hypertrophy of skeletal muscles: structural and functional aspects. *Acta Physiol* **188**, 77–89.
- Deban S (2003) Constraint and convergence in the evolution of salamander feeding. In: *Vertebrate Biomechanics and Evolution*. (eds Gasc JP, Casinos A, Bels VL), pp. 163–180. Oxford: BIOS Scientific Publishers.
- Deban S, Wake D (2000) Aquatic feeding in salamanders. In: *Feeding: Form, Function and Evolution in Tetrapod Vertebrates*. (ed. Schwenk K), pp. 65–94. San Diego: Academic.

- Denoël M** (2004) Terrestrial versus aquatic foraging in juvenile Alpine newts (*Triturus alpestris*). *Ecoscience* **11**, 404–409.
- Drüner L** (1902) Studien zur Anatomie der Zungenbein-, Kiemenbogen- und Kehlkopfmuskeln der Urodelen. I. Theil. *Zool Jahrb Abteil Anat* **15**, 435–622.
- Drüner L** (1904) Studien zur Anatomie der Zungenbein-, Kiemenbogen- und Kehlkopfmuskeln bei Urodelen. II. Theil. *Zool Jahrb Abteil Anat* **19**, 361–690.
- Findeis EK, Bemis WE** (1990) Functional morphology of tongue projection in *Taricha torosa* (Urodela: Salamandridae). *Zool J Linn Soc* **99**, 129–157.
- Flück M** (2006) Functional, structural and molecular plasticity of mammalian skeletal muscle in response to exercise stimuli. *J Exp Biol* **209**, 2239–2248.
- Folland JP, Williams AG** (2007) Morphological and neurological contributions to increased strength. *Sports Med* **37**, 145–168.
- Francis E** (1934) *The Anatomy of the Salamander*. Oxford: Clarendon Press.
- Gerth N, Sum S, Jackson S, et al.** (2009) Muscle plasticity of Inuit sled dogs in Greenland. *J Exp Biol* **212**, 1131–1139.
- Goldberg AL, Etlinger JD, Goldspink DF, et al.** (1974) Mechanism of work-induced hypertrophy of skeletal muscle. *Med Sci Sports* **7**, 185–198.
- Griffiths RA** (1997) *Newts and Salamanders of Europe*. London: Poyser Natural History.
- Halliday T** (1974) Sexual behaviour of the smooth newt, *Triturus vulgaris* (Urodela, Salamandridae). *J Herpetol* **8**, 277–292.
- Hanson AM, Stodieck LS, Cannon CM, et al.** (2010) Seven days of muscle re-loading and voluntary wheel running following hindlimb suspension in mice restores running performance, muscle morphology and metrics of fatigue but not muscle strength. *J Muscle Res Cell Motil* **31**, 141–153.
- Heiss E, Natchev N, Schwaha T, et al.** (2011) Oropharyngeal morphology in the basal tortoise *Manouria emys emys* with comments on form and function of the testudinid tongue. *J Morphol* **272**, 1217–1229.
- Heiss E, Aerts P, Van Wassenbergh S** (2013) Masters of change: seasonal plasticity in the prey-capture behavior of the Alpine newt *Ichthyosaura alpestris* (Salamandridae). *J Exp Biol* **216**, 4426–4434.
- Heiss E, Aerts P, Van Wassenbergh S** (2015) Flexibility is everything: prey capture throughout the seasonal habitat switches in the smooth newt *Lissotriton vulgaris*. *Org Divers Evol* **15**, 127–142.
- Hiiemae K** (2000) Feeding in mammals. In: *Feeding: Form, Function, and Evolution in Tetrapod Vertebrates*. (ed. Schwenk K), pp. 411–448. San Diego: Academic.
- Kiernan JA** (2003) *Histological and Histochemical Methods: Theory and Practice*. New York: Oxford University Press.
- Kleinteich T, Herzen J, Beckmann F, et al.** (2014) Anatomy, function, and evolution of jaw and hyobranchial muscles in cryptobranchoid salamander larvae. *J Morphol* **275**, 230–246.
- Kouzaki M, Masani K, Akima H, et al.** (2007) Effects of 20-day bed rest with and without strength training on postural sway during quiet standing. *Acta Physiol* **189**, 279–292.
- Larsen JH, Guthrie DJ** (1975) The feeding system of terrestrial tiger salamanders (*Ambystoma tigrinum melanostictum* Baird). *J Morphol* **147**, 137–153.
- Lauder GV, Reilly SM** (1988) Functional design of the feeding mechanism in salamanders: causal bases of ontogenetic changes in function. *J Exp Biol* **134**, 219–233.
- Lauder GV, Reilly SM** (1994) Amphibian feeding behavior: comparative biomechanics and evolution. In: *Biomechanics of Feeding in Vertebrates*. (eds Bels V, Chardon M, Vandewalle P), pp. 163–195. Berlin: Springer.
- Lauder GV, Shaffer HB** (1988) Ontogeny of functional design in tiger salamanders (*Ambystoma tigrinum*): are motor patterns conserved during major morphological transformations? *J Morphol* **197**, 249–268.
- Lieberman DE, Pearson OM, Polk JE, et al.** (2003) Optimization of bone growth and remodeling in response to loading in tapered mammalian limbs. *J Exp Biol* **206**, 3125–3138.
- Lüthi J, Howald H, Claassen H, et al.** (1986) Structural changes in skeletal muscle tissue with heavy-resistance exercise. *Int J Sports Med* **7**, 123–127.
- Matsuda JJ, Zernicke RF, Vailas AC, et al.** (1986) Structural and mechanical adaptation of immature bone to strenuous exercise. *J Appl Physiol* **60**, 2018–2034.
- Matthes E** (1934) Bau und Funktion der Lippensäule wasserlebender Urodelen. *Z Morphol Oekol Tiere* **28**, 155–169.
- Maughan RJ, Watson JS, Weit J** (1983) Strength and cross sectional area of human skeletal muscle. *J Physiol* **338**, 37–49.
- Metscher BD** (2009) MicroCT for comparative morphology: simple staining methods allow high-contrast 3D imaging of diverse non-mineralized animal tissues. *BMC Physiol* **9**, 11.
- Nauwelaerts S, Ramsay J, Aerts P** (2007) Morphological correlates of aquatic and terrestrial locomotion in a semi-aquatic frog, *Rana esculenta*: no evidence for a design conflict. *J Anat* **210**, 304–317.
- Nishikawa K** (2000) Feeding in frogs. In: *Feeding: Form, Function and Evolution in Tetrapod Vertebrates*. (ed. Schwenk K), pp. 117–147. San Diego: Academic.
- Nöllert A, Nöllert C** (1992) *Die Amphibien Europas: Bestimmung, Gefährdung, Schutz*. Stuttgart: Franckh-Kosmos.
- Nowell MM, Choi H, Rourke BC** (2011) Muscle plasticity in hibernating ground squirrels (*Spermophilus lateralis*) is induced by seasonal, but not low-temperature, mechanisms. *J Comp Physiol B* **181**, 147–164.
- O'Reilly J** (2000) Feeding in caecilians. In: *Feeding: Form, Function and Evolution in Tetrapod Vertebrates*. (ed. Schwenk K), pp. 149–166. San Diego: Academic.
- Özeti N, Wake DB** (1969) The morphology and evolution of the tongue and associated structures in salamanders and newts (family Salamandridae). *Copeia* **1**, 91–123.
- Piatt J** (1955) Regeneration of the spinal cord in the salamander. *J Exp Zool* **129**, 177–207.
- Reilly SM** (1987) Ontogeny of the hyobranchial apparatus in the salamanders *Ambystoma talpoideum* (Ambystomatidae) and *Notophthalmus viridescens* (Salamandridae): the ecological morphology of two neotenic strategies. *J Morphol* **191**, 205–214.
- Reilly SM, Lauder GV** (1990) Metamorphosis of cranial design in tiger salamanders (*Ambystoma tigrinum*): a morphometric analysis of ontogenetic change. *J Morphol* **204**, 121–137.
- Reilly SM, Lauder GV** (1992) Morphology, behavior, and evolution: comparative kinematics of aquatic feeding in salamanders. *Brain Behav Evol* **40**, 182–196.
- Romeis B** (1989) *Mikroskopische Technik*. München: Urban u. Schwarzenberg.
- Schwenk K** (2000a) Feeding in lepidosaurs. In: *Feeding: Form, Function and Evolution in Tetrapod Vertebrates*. (ed. Schwenk K), pp. 175–291. San Diego: Academic.

- Schwenk K** (2000b) An introduction to tetrapod feeding. In: *Feeding: Form, Function and Evolution in Tetrapod Vertebrates*. (ed. Schwenk K), pp. 21–61. San Diego: Academic.
- Shaffer H, Lauder G** (1988) The ontogeny of functional design: metamorphosis of feeding behaviour in the tiger salamander (*Ambystoma tigrinum*). *J Zool* **216**, 437–454.
- Skorczewski T, Cheer A, Wainwright PC** (2012) The benefits of planar circular mouths on suction feeding performance. *J R Soc Interface* **9**, 1767–1773.
- Stocum DL, Dearlove GE** (1972) Epidermal-mesodermal interaction during morphogenesis of the limb regeneration blastema in larval salamanders. *J Exp Zool* **181**, 49–61.
- Thiesmeier B, Schulte U** (2010) *Der Bergmolch: im Flachland wie im Hochgebirge zu Hause*. Bielefeld: Laurenti.
- Wake DB, Deban SM** (2000) Terrestrial feeding in salamanders. In: *Feeding: Form, Function and Evolution in Tetrapod Vertebrates*. (ed. Schwenk K), pp. 95–116. San Diego: Academic.
- Warburg M, Rosenberg M** (1997) Ultrastructure of ventral epidermis in the terrestrial and aquatic phases of the newt *Triturus vittatus* (Jenyns). *Ann Anat* **179**, 341–347.
- Yokoyama H** (2008) Initiation of limb regeneration: the critical steps for regenerative capacity. *Dev Growth Differ* **50**, 13–22.